Nanoscale channels on ectomycorrhizal-colonized chlorite: Evidence for plant-driven fungal dissolution

Salvatore A. Gazzè,[1] Loredana Saccone,[1,2] K. Vala Ragnarsdottir,[3] Mark M. Smits,[4] Adele L. Duran,[5] Jonathan R. Leake,[5] Steven A. Banwart,[6] and Terence J. McMaster[1,7]

Received 3 March 2012; revised 18 June 2012; accepted 23 June 2012; published 18 August 2012.

[1] The roots of many trees in temperate and boreal forests are sheathed with ectomycorrhizal fungi (EMF) that extend into the soil, forming intimate contact with soil minerals, from which they absorb nutrient elements required by the plants and, in return, are supported by the organic carbon photosynthesized by the trees. While EMF are strongly implicated in mineral weathering, their effects on mineral surfaces at the nanoscale are less documented. In the present study, we investigated the effects of symbiotic EMF on the topography of a chlorite mineral using atomic force microscopy. A cleaning protocol was successfully applied to remove fungal hyphae without altering the underlying mineral structure and topography. Examination of the exposed chlorite surface showed the presence of primary channels, of the order of a micron in width and up to 50 nm in depth, the morphology of which strongly indicates a fungal-induced origin. Smaller secondary channels were observed extending from the primary channels and would appear to be involved in their enlargement. The presence of channels is the first nanoscale demonstration of the effects of fungal interaction, fuelled by plant photosynthate, on the topography of a chlorite mineral, and it provides clear evidence of the ability of EMF to enhance mineral dissolution.

Citation: Gazzè, S. A., L. Saccone, K. Vala Ragnarsdottir, M. M. Smits, A. L. Duran, J. R. Leake, S. A. Banwart, and T. J. McMaster (2012), Nanoscale channels on ectomycorrhizal-colonized chlorite: Evidence for plant-driven fungal dissolution, *J. Geophys. Res.*, *117*, G00N09, doi:10.1029/2012JG002016.

1. Introduction

[2] Mineral weathering is a fundamental geochemical process within the Earth Critical Zone (CZ) that provides most of the essential elements required by terrestrial ecosystems., The process plays a primary role both in soil formation and in the control of atmospheric CO_2 over geochemical carbon cycle time-scales [*Brantley et al.*, 2007]. The CZ is defined as "the heterogeneous, near-surface environment in which complex interactions involving rock, soil, water, air, and living organisms regulate the natural habitat and determine the availability of life-sustaining resources" [*National Research Council*, 2001].

[3] Plants, the root systems and associated soil microorganisms are the main biotic factors that accelerate mineral weathering [*Banfield et al.*, 1999; *Barker et al.*, 1998; *Taylor et al.*, 2009]. The actions of organisms in the dissolution of minerals normally requires the use of organic compounds as energy sources by the organisms. The availability of these chemical energy sources controls the biomass of organisms and the extent to which they may be able to chemically and physically alter minerals [*Leake et al.*, 2008]. Among soil organisms, ectomycorrhizal fungi (EMF) are provided with an unusually large and persistent source of chemical energy by forming symbiotic associations with the roots of trees through which they obtain between a quarter and a third of the total photosynthate formed by trees in boreal forest ecosystems [*Leake et al.*, 2004]. EMF use this for growth, accelerating mineral weathering and the absorption of nutrient elements required by themselves and their host plants [*Yuan et al.*, 2004]. Hyphae, the EMF functional units for surface exploration and nutrient uptake, are long, tubular structures, with a diameter of few micrometres, which in the case of EMF, form dense mats of filaments in soils, with about 200 km of fungal mycelium per kg of soil in boreal forests [*Leake et al.*, 2004].

[4] The weathering effects on minerals due to fungi, and microorganisms in general, have been reported in several

[1]H. H. Wills Physics Laboratory, University of Bristol, Bristol, UK.
[2]Now at Institute of Forest Products Research, Edinburgh Napier University, Edinburgh, UK.
[3]Institute of Earth Sciences, School of Engineering and Natural Sciences, University of Iceland, Reykjavík, Iceland.
[4]Department of Environmental Biology, Hasselt University, Diepenbeek, Belgium.
[5]Department of Animal and Plant Sciences, Alfred Denny Building, University of Sheffield, Sheffield, UK.
[6]Department of Civil and Structural Engineering, Kroto Research Institute, North Campus, University of Sheffield, Sheffield, UK.
[7]Bristol Centre for Functional Nanomaterials, University of Bristol, Bristol, UK.

Corresponding author: T. J. McMaster, Bristol Centre for Functional Nanomaterials, University of Bristol, Bristol BS8 1FD, UK. (t.mcmaster@bristol.ac.uk)

©2012. American Geophysical Union. All Rights Reserved.
0148-0227/12/2012JG002016

Table 1. Elemental Composition of Chlorite and Agar Composition for the Microcosm

Mineral	Microcosm (–Fe)
Concentration (mmol L^{-1})	
$Ca(NO_3)_2$	0.075
$MgSO_4$	0.256
K_2HPO_4	1.0
KCl	1.0
$(NH_4)_2SO_4$	1.73
$MnSO_4$	0.009
H_3BO_4	0.05
$(NH_4)_6Mo_7O_{24}$	0.00015
$ZnSO_4$	0.0015
$CuSO_4$	0.0015
$(NH_4)_2HPO_4$	1.16
Concentration (g L^{-1})	
Agar	15

studies, in which mineral dissolution has often been studied in terms of microbial extraction of elements from the minerals [*Barker et al.*, 1997; *Hopf et al.*, 2009; *Paris et al.*, 1995; *Yuan et al.*, 2004]. In contrast, knowledge of localized alterations of the mineral surface caused by the direct contact with the microorganism is more limited. This is an important aspect given that weathering reactions are mediated by the physical attachment of microbes to minerals, and thereby the interfacial area is likely to be the most severely affected [*Bonneville et al.*, 2009].

[5] In the case of EMF, for example, their capability to physically alter mineral surfaces is still a topic of debate [*Jongmans et al.*, 1997; *Sverdrup*, 2009]. In previous studies tubular tunnels in forested podzol soils, containing plagioclase feldspar and hornblende, were observed [*Finlay*, 2008; *Jongmans et al.*, 1997; *van Breemen et al.*, 2000], and while their origin was not fully established, it was speculated that EMF could have been responsible for their creation [*Finlay*, 2008]. On the contrary, abiotic factors have also been proposed to be responsible for these tunnels, as similar features have been observed in Antarctica and in Arctic areas where no fungi have been present for the last ten million years [*Sverdrup*, 2009]. As regards laboratory studies, dissolution channels on biotite flakes have been reported on systems where the flakes were in contact with microorganisms (non-symbiotic EMF alone and symbiotic EMF plus bacteria), growth medium, water and plant roots [*Balogh-Brunstad et al.*, 2008a, 2008b]; in these studies, fungi were thought to be responsible for some of the dissolution features, while others were attributed to bacteria and root tips [*Balogh-Brunstad et al.*, 2008a]. In a recent study, *Bonneville et al.* [2009] showed that, at the symbiotic EMF-biotite interface, the biotite presented altered sub-surface spacings, depletion of K and the oxidation of the iron from Fe (II) to Fe (III).

[6] Here the direct action of EMF on chlorite was investigated by obtaining nanoscale resolution 3-dimensional images of the effects of symbiotic EMF on chlorite using atomic force microscopy (AFM). In order to remove the possibility of other biotic (such as bacteria, other fungal species and root hairs and tips) and/or abiotic (notably water) weathering effects on chlorite flakes, in this set-up the chlorite surface was exposed to air, and not liquid, and only in contact with the symbiotic EMF *Paxillus involutus.* Chlorite is a phyllosilicate mineral common in soils [*Glowa et al.*, 2003; *Martin*, 1954] which contains important cations for fungal and plant nutritional requirements, such as Mg and Fe, but the possible presence of biogenic signatures on its structure has never been studied, as most laboratory studies have used the more-weatherable biotite as a substrate [*Balogh-Brunstad et al.*, 2008a, 2008b; *Bonneville et al.*, 2009]. Importantly, in the study presented here, the fungi were grown in symbiotic association with a tree seedling, as in nature, where the only energy supply for EMF is represented by the plant photosynthate products.

2. Materials and Methods

2.1. Microcosm

[7] A detailed description of the general microcosm setting and growth conditions has been described previously [*Saccone et al.*, 2011]. Briefly, the axenic microcosm consisted of 10 cm square Petri dishes with nutrient agar lacking Fe (Table 1), on top of which a single-grain-thickness bed of acid-washed and sieved perlite was deposited. Iron was deliberately omitted from the nutrient agar to induce Fe limitation and stimulate fungal colonization of Fe-bearing minerals. A *Pinus sylvestris* seedling with mycorrhizal *P. involutus* cultured under aseptic conditions was transferred to the Petri dish, with the shoots protruding through a hole, covered with sterilized lanolin (Figure 1a). On top of the perlite bed four polypropylene wells, containing a layer of perlite, were positioned to provide discrete weathering arenas. The microcosm was maintained for seven months inside environmental chambers under the following conditions. Daytime (06:00–23:59): temperature at 15°C, 60% humidity, CO_2 at ambient levels and photon flux density of 388 μmol m^{-2} s^{-1}. Overnight (24:00–05:59): temperature at 10°C, 75% humidity, CO_2 at ambient levels and no light.

2.2. Mineral Samples

[8] The mineral sample was a chlorite and the empirical formula was determined with Electron Probe Micro Analysis (EPMA) to be $(Mg_{9.79}Fe_{0.62}Mn_{0.01}Al_{1.47}Ca_{0.01}Na_{0.01}Cr_{0.01}F_{0.01})(Si_{6.67}Al_{1.33})O_{20}(OH)_{16}$. The flakes were cleaved with adhesive tape on the (001) face to expose the surface to be imaged with AFM, and sterilized through two autoclaving cycles at 121°C for 12 min. In the microcosm, two chlorite flakes were positioned inside the polypropylene wells, which provide a hydrophobic barrier between the plant root compartment over which the EMF can grow so that the interaction between the minerals and EMF does not involve any direct contact with root tips. One polypropylene well was positioned close to the roots plus hyphae system, while the other was placed more remotely as shown in Figure 1a. This was done in order to limit fungal colonization for the remotely positioned flake and test the effectiveness and invasiveness of the cleaning protocol (described below), without the possible effects of fungi on the chlorite surface.

[9] The chlorite (001) surface that was analyzed with AFM was that exposed to the air and not that in contact with the perlite bed in the wells; therefore it has been solely in contact with the fungus. At the end of the seven-month incubation period, one chlorite flake was well-colonized, Figure 1b, while the one positioned far from the shoots had

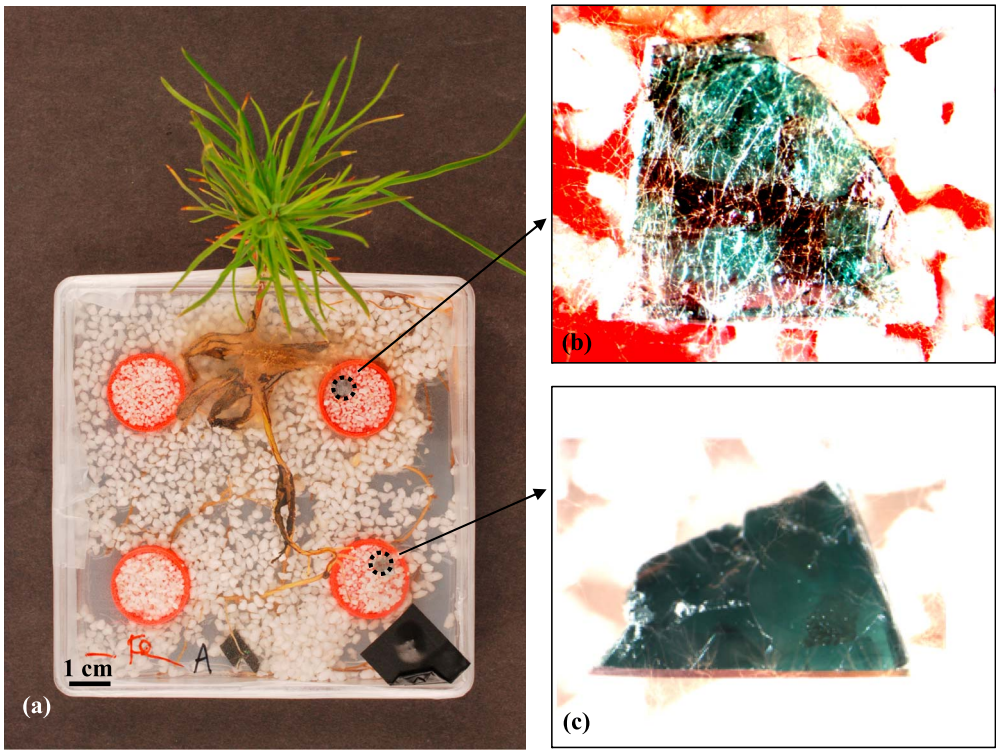

Figure 1. (a) In the axenic microcosm, *P. sylvestris* roots are in symbiosis with *P. involutus.* Two chlorite flakes are positioned in the circular wells, with (b) one flake well colonized while (c) the other is almost devoid of hyphae.

almost no hyphal colonization, Figure 1c, except for a few hyphae along the edges. During sample handling and analysis, the (001) surface of the flakes was not touched except during the cleaning procedure.

2.3. Cleaning Protocol of a Chlorite Flake

[10] The cleaning protocol consisted in immersion of the chlorite flakes in a stirred bath of 2% Sodium Dodecyl Sulphate (SDS, Sigma-Aldrich) at 50°C for 1 h, followed by gentle wiping of the mineral surface with a lens tissue immersed in 2% SDS solution, rinsing with ultrapure Fluka water, and drying under an oxygen-free N_2 stream.

2.4. Tapping Mode Atomic Force Microscopy (TM-AFM)

[11] A Bruker AXS Dimension AFM (Santa Barbara, CA) was used with Arrow-NCR-W cantilevers from Nanoworld (Neuchâtel, Switzerland), with a nominal spring constant of 42 N/m (Manufacturer's data). The microscope was operated in tapping mode in air at piezo drive frequencies around 280 kHz, and at free amplitude of cantilever oscillation of 1 V. For normal imaging, setpoint control amplitudes of 0.7–0.9 V and a scan rate of 1 Hz were used. Two spatially correlated data sets were simultaneously obtained: namely height data and cantilever phase angle data [*Saccone et al.*, 2011]. In height mode, the sample topography was recorded, while in cantilever phase angle mode, the oscillation phase lag of the cantilever response signal compared with the driving oscillation of the cantilever was recorded. Offline processing consisted of low-order flattening, plane-fitting and proprietary image analysis subroutines NanoScope 5.30r1 (Bruker AXS, USA).

3. Results

3.1. Cleaning

[12] The effectiveness of the cleaning was evaluated on the chlorite flake of Figure 1c, by comparing the topography of the same (001) areas before its introduction in the microcosm and after its incubation inside the microcosm and subsequent cleaning (using the protocol described in section 2.3). The procedure described in *Saccone et al.* [2011] was used to identify the same, micrometre-scale areas with AFM after a time interval of several months. Ten different chlorite areas, ranging in area from 12 μm^2 to 10000 μm^2, have been imaged, with a typical example shown in Figure 2. The cleaning process did not degrade the underlying chlorite mineral structure, as can be seen in a comparison of the same areas before the introduction of the chlorite flake into the microcosm, Figure 2a, and after microcosm incubation and cleaning, Figure 2b. It is known that high-energy step edges are more susceptible to damage and weathering [*Kalinowski and Schweda*, 1996; *Turpault and Trotignon*, 1994], and the integrity of the observed step edges after cleaning indicate that the cleaning protocol was not damaging the mineral topography. There are some particles present in the "after–cleaning" image, Figure 2b, however the overall surface topography and step-edge morphology appears unaltered, without etch pits and other clear weathering effects.

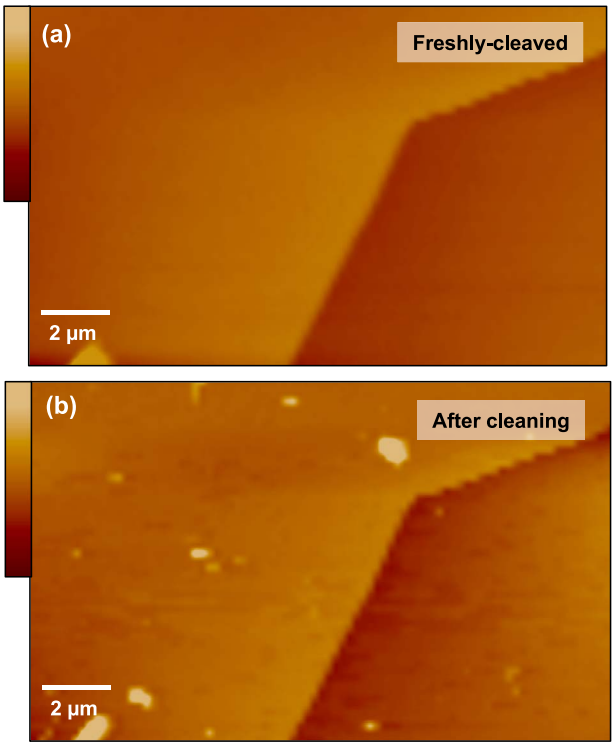

Figure 2. (a) A freshly cleaved chlorite area. (b) The same chlorite areas after the flake has been incubated in the microcosm. The surface displays the same crystallographic steps, and no weathering effect is visible. The Z-height scale is 0–15 nm.

3.2. Nanoscale Channels in the Chlorite

[13] AFM analysis of the chlorite flake colonized by EMF, Figure 1b, and after removal of the colonizing hyphae as described in section 3.1, revealed the presence of channels within a single scan area, Figure 3. In an area of about 47,000 μm^2 a total length of 900 μm of channels was observed, displaying widths from 0.4 to 3 μm and depths from 1.4 nm (equivalent to a single chlorite unit cell c-axis repeat spacing) to about 50 nm. Two examples of topographic images of channels, with accompanying height profiles across the channels, are displayed in Figures 4a and 4b. A strong indication of the fungal origin for the observed channels was their resemblance in outline and growth pattern to the surface-colonizing hyphae (Figures 4c and 4d). The growth modes of the hyphae were characterized by: (i) both straight and meandering outlines, the latter most likely as a response of surface irregularities, oxygen gradients, and the effect of neighboring hyphae [*Gooday*, 1995]; and (ii) the formation of branches, presumably for more extensive surface exploration [*Dynesen and Nielsen*, 2003]. For example, Figures 4a and 4b show, respectively, a channel with a V-shaped contour and the termination of a meandering 1 μm-wide 1.5 nm-deep channel, with comparable fungal outlines displayed in Figures 4c and 4d, respectively. Channel branching has also been observed, and just as the channel contours resemble the contours of individual hyphae, the branching matches that of the hyphae branching.

3.3. High-Resolution External Channel Structure

[14] Inspecting the branch point in more detail, it can be seen in Figure 5a that the channel of the branch from center left to top right, emanating from the main channel, is

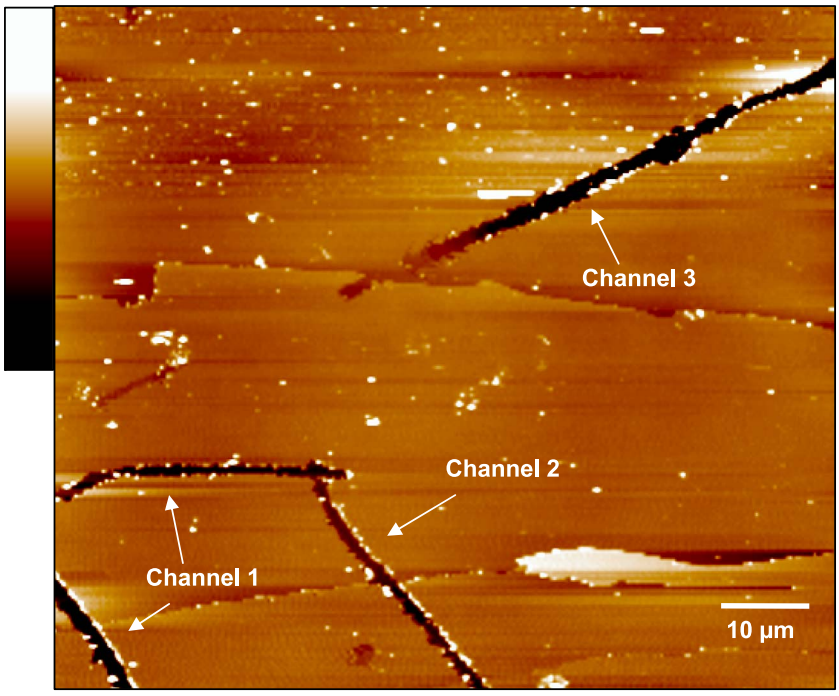

Figure 3. A (001) chlorite area displaying the typical channels produced on the chlorite surface after colonization by hyphae. The Z-height scale is 0–30 nm.

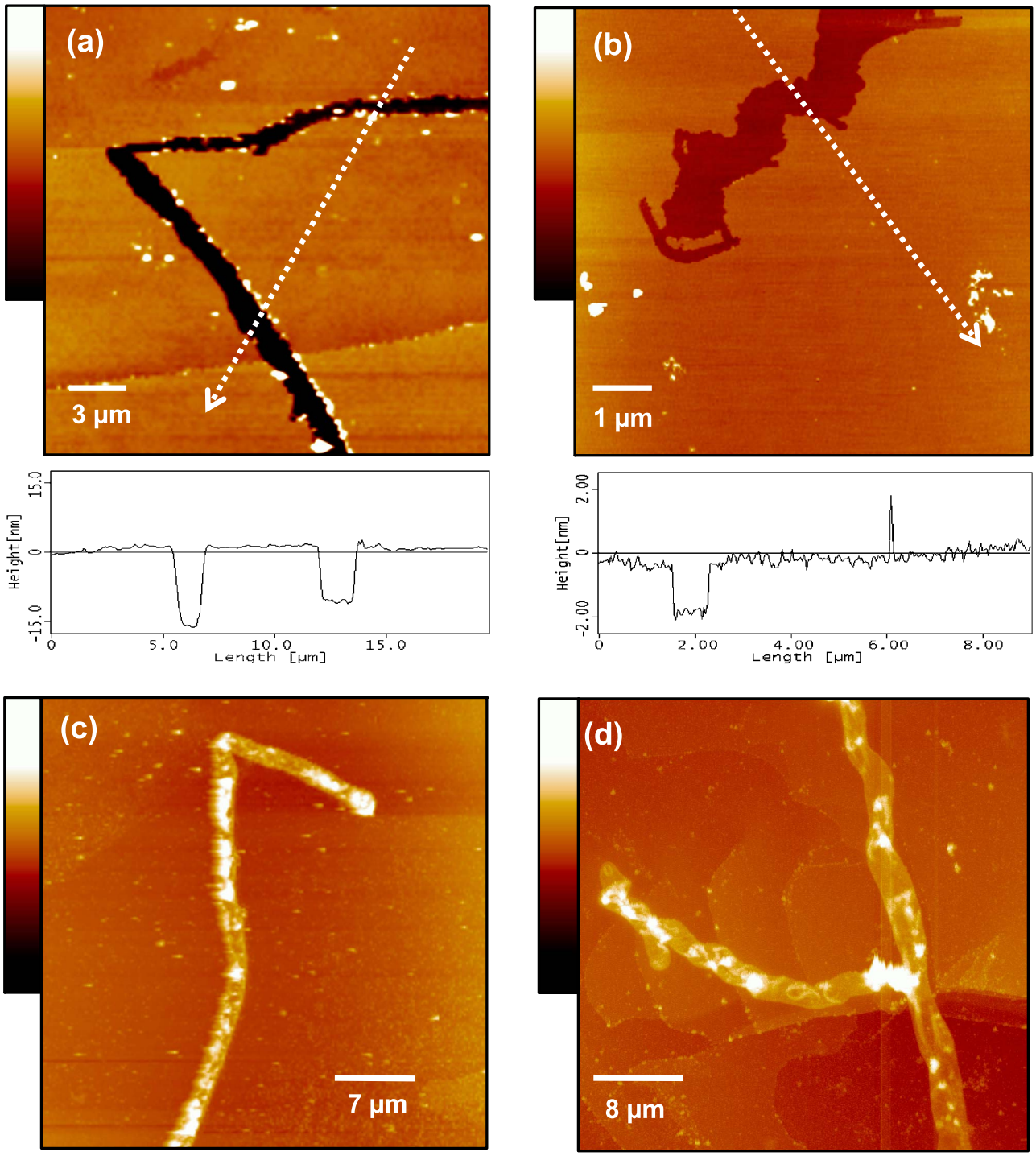

Figure 4. Typical channel shapes and accompanying line profiles, with widths between 0.4 and 1.5 μm and depths of up to 15 nm. (a, b) Line profiles are measured along the dotted arrows, in which the arrowed end is the left hand side of the respective profile. (c, d) Hyphal outlines on the colonized (uncleaned) samples, showing morphologies similar to those of the channel. Z-height scales are (a) 0–20 nm, (b) 0–10 nm, (c) 0–500 nm, and (d) 0–1500 nm.

shallower than the main channel. Shorter, secondary channels were often observed to spread from the edges of primary channels (Figures 5a and 5b), both main and branched, producing a characteristic "herringbone" texture. Observing the secondary channels in Figure 5a, they orient toward the growth direction of the hypha with an average spacing of 0.8 μm. Progressively, larger secondary channels that sometimes coalesce with the main channel can be observed, as highlighted in Figures 5a and 5b.

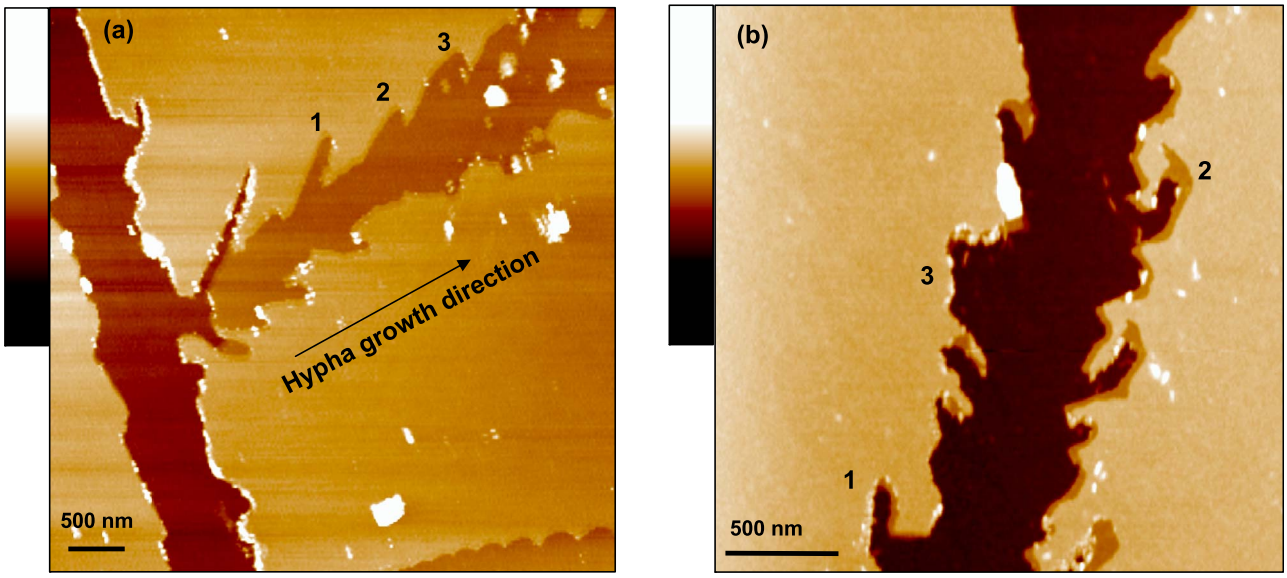

Figure 5. Two examples of the herringbone texture associated with some of the hyphal channels: (a, b) secondary channels oriented along the growth direction of the hyphal branch, with various stages of secondary channel evolution present (indicated by numbers) and showing progressive expansion, for example numbers 1, 2 and 3 in Figure 5a. Secondary channel number 3 in Figure 5b shows channel enlargement and coalescence with the main channel. Z-height scales: (a) 0–17 nm, (b) 0–20.

3.4. High-Resolution Internal Channel Topography

[15] Further evidence of a fungal origin for channel formation is the residual non-chlorite material that is sometimes visible in the channels, after incomplete cleaning (Figure 6). The AFM cantilever phase angle data is sensitive to material composition and properties [*Schmitz et al.*, 1997; *Saccone et al.*, 2011]. The phase angle signal indicates a residue of material along the edges and inside the channel (lighter in color) that is not chlorite, and could be remnants of hyphal surface coat material, or hyphal exudates. Within the channel, the mineral surface shows evidence of severe localized surface disruption in the form of many step edges, which are not present outside the hyphal boundary on the chlorite immediately bordering the channel, and which could be the result of hyphal weathering activity.

4. Discussion

[16] The capability of EMF to physically alter minerals in natural-like conditions within the CZ is still an open topic. Here a high-resolution imaging technique, AFM, was used with the advantages of analyzing samples in their natural state, with no image-inducing alteration of its surface properties. This technique was applied to image a common soil mineral, chlorite, which had been in contact with symbiotic EMF *P. involutus* for seven months in an axenic microcosm.

[17] It was necessary to remove hyphae and their exudates from the mineral surface, in order to inspect for possible weathering effects caused by the EMF. A specific cleaning procedure was tested on a chlorite flake that had been incubated in the microcosm, but with almost no hypha on it (Figure 1c) in order to distinguish potential destructive effects of the cleaning from the weathering activity of the fungus. The applied cleaning protocol did not alter the topography of the mineral chlorite visualized at high resolution and, most significantly, did not introduce any weathering features such as etch pits and surface cracks that could be erroneously attributed to biogenic weathering (Figure 2). The observed dissolution features on EMF-colonized chlorite flakes

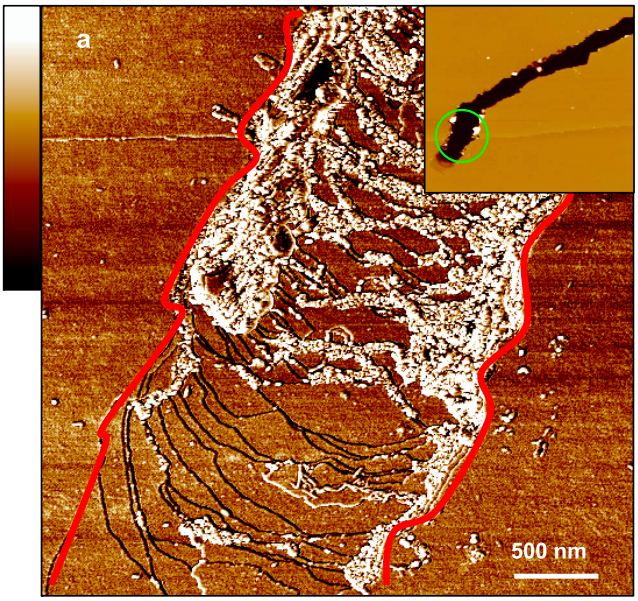

Figure 6. The edges of the channel are highlighted in red. The location of the area is circled in the inset. Inside the channel multiple step edges are present compared to outside the channel. Isolated single steps are often seen on freshly cleaved chlorite (see, for example, Figure 1), but the multi-step morphology seen in this channel is not observed on freshly cleaved samples. Non-mineral material (lighter in color) is present as small particles inside the channel. The Z-phase scale is 0°–20°.

(Figure 3) can therefore be attributed only to the weathering activity of EMF hyphae. High resolution imaging of channels provided evidence that strengthens this hypothesis, such as the similarity between channels and hyphae outlines, as in Figure 4, and the evidence of weathered chlorite inside the channel outline, as shown in Figure 6.

[18] In a possible model of channel formation, the process would start with the formation of a narrow channel and then the activity of hypha leads to a progressive enlargement of it. This is supported by the branching displayed in Figure 5a, where the branched channel is narrower and shallower than the main hypha channel, as expected, since the branching hypha will have had less contact (and thus weathering) time with the chlorite. The enlargement of the channels could take place via the production, expansion and coalescence of the secondary channels seen in the herringbone textures, as indicated by numbers 1, 2 and 3 in Figures 5a and 5b.

[19] During the growth phase, the cell wall close to the tip becomes more permeable as it has to allow the expansion of the fungal tip, and this permeability allows a higher secretion of fungal exudates and weathering agents (such as oxalate) [*Bartnicki-Garcia et al.*, 2000; *Gooday*, 1996; *Sun et al.*, 1999]. These exudates attack and weaken the underlying mineral structure, thus contributing to and/or determining the formation of channels. In a recent study, *Saccone et al.* [2011] have demonstrated that the surface of hornblende colonized by symbiotic *P. involutus* in similar microcosm settings is extensively covered by a layer of fungal exudates and that the latter weakens the underlying mineral structure. Calcium oxalate was also detected on the surface of *P. involutus* when in contact with Ca-rich minerals [*Schmalenberger et al.*, 2009].

[20] Together with the chemical attack of minerals, the physical contact of the hypha may play a role in channel formation as well. Internal pressure in hyphae can reach values between 0.4 and 8 MPa, and has been implicated in structural alterations of phyllosilicates [*Bonneville et al.*, 2009], possibly by causing strain in the mineral during hyphal growth. This might have had a role to play in channel formation, particularly when the mineral surface is already weakened by the presence of a layer of exudates.

[21] Hypothesizing the mechanism involved in the formation of the herringbone texture, is informed by the known growth behavior of hyphae. Hyphal tips have been reported to elongate in a pulsed way, alternating periods of slow and fast growth [*Lopez-Franco et al.*, 1994]. According to the data provided for different fungal species [*Lopez-Franco et al.*, 1994], the growth length during a single pulse ranges from 0.28 to 3.22 μm. The secondary channels observed here have an average spacing of 0.8 μm, within the range of the observed growth pulses, and therefore their formation could be associated with the phase of a pulse and be determined by an higher secretion of weathering agents, perhaps coupled with the strain stress exerted on the mineral surface during the pulsed growth.

5. Conclusions

[22] The experimental design restricted the variables in the observed weathering features to the symbiotic EMF alone, excluding the involvement of other elements, such as water and other abiotic factors that could mask the active role of EMF in physically altering minerals. It has been demonstrated that EMF, using only the energy provided by the plant roots as in nature, are able to weather minerals, such as chlorite, that are more stable than the commonly used biotite for laboratory studies [*Hamer et al.*, 2003]. In particular, at the pH values commonly present in bulk soil solution, approximately 4–5 [*Arocena and Glowa*, 2000; *Shen et al.*, 1996], chlorite presents weathering rates comparable to hornblende and plagioclase feldspars, of the order of 10^{-12}-10^{-13} mol m^{-2} s^{-1} [*Alekseyev*, 2007; *Bandstra et al.*, 2008; *Lowson et al.*, 2005]. Therefore, the results presented here support the hypothesis that the ectomycorrhizal fungi may be implicated in the widespread tubular tunnels first observed by *Jongmans et al.* [1997] in plagioclase feldspar and hornblende minerals in forested podzol soils in the Critical Zone. This is the first time that the structure of fungi-linked channels have been characterized at the nanoscale. AFM images have shown that channels often display a "herringbone" structure, characterized by secondary, lateral channels that could be involved in the enlargement of the main channels. The precise mechanisms involved in channel formation and evolution are uncertain, although chemical (production of oxalate and other fungal exudates) and physical components (pressure exerted by hypha) may play a cooperative role.

[23] **Acknowledgments.** This research was undertaken within the framework of the Marie Curie Early Stage Training project "MISSION" (Mineral Surface Science for Nanotechnology) (MEST-CT-2005-020828) and of the NERC-funded integrated project "Biological Weathering in Earth Systems" (grant NE/C004566/1), which is a collaboration among the universities of Bristol, Sheffield, and Leeds.

References

Alekseyev, V. A. (2007), Equations for the dissolution reaction rates of montmorillonite, illite, and chlorite, *Geochem. Int.*, *45*(8), 770–780, doi:10.1134/S0016702907080046.

Arocena, J. M., and K. R. Glowa (2000), Mineral weathering in ectomycorrhizosphere of subalpine fir (*Abies lasiocarpa* (Hook.) Nutt.) as revealed by soil solution composition, *For. Ecol. Manage.*, *133*(1–2), 61–70, doi:10.1016/S0378-1127(99)00298-4.

Balogh-Brunstad, Z., C. K. Keller, R. A. Gill, B. T. Bormann, and C. Y. Li (2008a), The effect of bacteria and fungi on chemical weathering and chemical denudation fluxes in pine growth experiments, *Biogeochemistry*, *88*(2), 153–167, doi:10.1007/s10533-008-9202-y.

Balogh-Brunstad, Z., C. K. Keller, J. T. Dickinson, F. Stevens, C. Y. Li, and B. T. Bormann (2008b), Biotite weathering and nutrient uptake by ectomycorrhizal fungus, *Suillus tomentosus*, in liquid-culture experiments, *Geochim. Cosmochim. Acta*, *72*(11), 2601–2618, doi:10.1016/j.gca.2008.04.003.

Bandstra, J. Z., H. L. Buss, R. K. Campen, L. J. Liermann, J. Moore, E. M. Hausrath, A. K. Navarre-Sitchler, J. Jang, and S. L. Brantley (2008), Appendix: Compilation of mineral dissolution rates, in *Kinetics of Water-Rock Interactions*, edited by S. L. Brantley et al., pp. 737–823, Springer, New York.

Banfield, J. F., W. W. Barker, S. A. Welch, and A. Taunton (1999), Biological impact on mineral dissolution: Application of the lichen model to understanding mineral weathering in the rhizosphere, *Proc. Natl. Acad. Sci. U. S. A.*, *96*(7), 3404–3411, doi:10.1073/pnas.96.7.3404.

Barker, W. W., S. A. Welch, and J. F. Banfield (1997), Biogeochemical weathering of silicate minerals, *Rev. Mineral. Geochem.*, *35*, 391–428.

Barker, W. W., S. A. Welch, S. Chu, and J. F. Banfield (1998), Experimental observations of the effects of bacteria on aluminosilicate weathering, *Am. Mineral.*, *83*(11–12), 1551–1563.

Bartnicki-Garcia, S., C. E. Bracker, G. Gierz, R. Lopez-Franco, and H. S. Lu (2000), Mapping the growth of fungal hyphae: Orthogonal cell wall expansion during tip growth and the role of turgor, *Biophys. J.*, *79*(5), 2382–2390, doi:10.1016/S0006-3495(00)76483-6.

Bonneville, S., M. M. Smits, A. Brown, J. Harrington, J. R. Leake, R. Brydson, and L. G. Benning (2009), Plant-driven fungal weathering: Early stages of mineral alteration at the nanometer scale, *Geology*, *37*(7), 615–618, doi:10.1130/G25699A.1.

Brantley, S. L., M. B. Goldhaber, and K. Vala Ragnarsdottir (2007), Crossing disciplines and scales to understand the Critical Zone, *Elements*, *3*, 307–314, doi:10.2113/gselements.3.5.307.

Dynesen, J., and J. Nielsen (2003), Branching is coordinated with mitosis in growing hyphae of Aspergillus nidulans, *Fungal Genet. Biol.*, *40*(1), 15–24, doi:10.1016/S1087-1845(03)00053-7.

Finlay, R. D. (2008), Ecological aspects of mycorrhizal symbiosis: With special emphasis on the functional diversity of interactions involving the extraradical mycelium, *J. Exp. Bot.*, *59*(5), 1115–1126, doi:10.1093/jxb/ern059.

Glowa, K. R., J. M. Arocena, and H. B. Massicotte (2003), Extraction of potassium and/or magnesium from selected soil minerals by Piloderma, *Geomicrobiol. J.*, *20*(2), 99–111, doi:10.1080/01490450303881.

Gooday, G. W. (1995), The dynamics of hyphal growth, *Mycol. Res.*, *99*, 385–394, doi:10.1016/S0953-7562(09)80634-5.

Gooday, G. W. (1996), Cell walls, in *The Growing Fungus*, edited by N. A. R. Gow and G. M. Gadd, pp. 43–62, Chapman and Hall, London.

Hamer, M., R. C. Graham, C. Amrhein, and K. N. Bozhilov (2003), Dissolution of ripidolite (Mg, Fe-Chlorite) in organic and inorganic acid solutions, *Soil Sci. Soc. Am. J.*, *67*, 654–661, doi:10.2136/sssaj2003.0654.

Hopf, J., F. Langenhorst, K. Pollok, D. Merten, and E. Kothe (2009), Influence of microorganisms on biotite dissolution: An experimental approach, *Chem. Erde Geochem.*, *69*, 45–56, doi:10.1016/j.chemer.2008.11.001.

Jongmans, A. G., N. van Breemen, U. Lundström, P. A. W. van Hees, R. D. Finlay, M. Srinivasan, T. Unestam, R. Giesler, P.-A. Melkerud, and M. Olsson (1997), Rock-eating fungi, *Nature*, *389*, 682–683, doi:10.1038/39493.

Kalinowski, B. E., and P. Schweda (1996), Kinetics of muscovite, phlogopite, and biotite dissolution and alteration at pH 1–4, room temperature, *Geochim. Cosmochim. Acta*, *60*(3), 367–385, doi:10.1016/0016-7037(95)00411-4.

Leake, J. R., D. Johnson, D. Donnelly, G. Muckle, L. Boddy, and D. Read (2004), Networks of power and influence: The role of mycorrhizal mycelium in controlling plant communities and agroecosystem functioning, *Can. J. Bot.*, *82*(8), 1016–1045, doi:10.1139/b04-060.

Leake, J. R., A. L. Duran, K. E. Hardy, I. Johnson, D. J. Beerling, S. A. Banwart, and M. M. Smits (2008), Biological weathering in soil: The role of symbiotic root-associated fungi biosensing minerals and directing phiotosynthate-energy into grain-scale mineral weathering, *Mineral. Mag.*, *72*(1), 85–89, doi:10.1180/minmag.2008.072.1.85.

Lopez-Franco, R., S. Bartnicki-Garcia, and C. E. Bracker (1994), Pulsed growth of fungal hyphal tips, *Proc. Natl. Acad. Sci. U. S. A.*, *91*(25), 12,228–12,232, doi:10.1073/pnas.91.25.12228.

Lowson, R. T., M. C. J. Comarmond, G. Rajaratnam, and P. L. Brown (2005), The kinetics of the dissolution of chlorite as a function of pH and at 25°C, *Geochim. Cosmochim. Acta*, *69*(7), 1687–1699, doi:10.1016/j.gca.2004.09.028.

Martin, R. T. (1954), Clay minerals of five New York soil profiles, *Soil Sci.*, *77*(5), 389–400, doi:10.1097/00010694-195405000-00005.

National Research Council (2001), *Basic Research Opportunities in Earth Science*, 154 pp., Natl. Acad. Press, Washington, D. C.

Paris, F., P. Bonnaud, J. Ranger, and F. Lapeyrie (1995), In vitro weathering of phlogopite by ectomycorrhizal fungi: 1. Effect of K+ and Mg2+ deficiency on phyllosilicate evolution, *Plant Soil*, *177*(2), 191–201, doi:10.1007/BF00010125.

Saccone, L., S. A. Gazzè, A. L. Duran, J. R. Leake, S. A. Banwart, K. Vala Ragnarsdottir, M. M. Smits, and T. J. McMaster (2011), High-resolution characterization of ectomycorrhizal fungal-mineral interactions in axenic microcosm experiments, *Biogeochemistry*, doi:10.1007/s10533-011-9667-y, in press.

Schmalenberger, A., A. L. Duran, J. R. Leake, M. E. Romero-Gonzales, and S. A. Banwart (2009), Mineralogy controls oxalic acid release in mycorrhiza weathering, *Geochim. Cosmochim. Acta*, *73*(13), A1177.

Schmitz, I., M. Schreiner, G. Friedbacher, and M. Grasserbauer (1997), Phase imaging as an extension to tapping mode AFM for the identification of material properties on humidity-sensitive surfaces, *Appl. Surf. Sci.*, *115*(2), 190–198, doi:10.1016/S0169-4332(97)80204-8.

Shen, Y., L. Ström, J. A. Jönsson, and G. Tyler (1996), Low-molecular organic acids in the rhizosphere soil solution of beech forest (*Fagus sylvatica* L.) cambisols determined by ion chromatography using supported liquid membrane enrichment technique, *Soil Biol. Biochem.*, *28*(9), 1163–1169, doi:10.1016/0038-0717(96)00119-8.

Sun, Y. P., T. Unestam, S. D. Lucas, K. J. Johanson, L. Kenne, and R. Finlay (1999), Exudation-reabsorption in a mycorrhizal fungus, the dynamic interface for interaction with soil and soil microorganisms, *Mycorrhiza*, *9*(3), 137–144, doi:10.1007/s005720050298.

Sverdrup, H. (2009), Chemical weathering of soil minerals and the role of biological processes, *Fungal Biol. Rev.*, *23*(4), 94–100, doi:10.1016/j.fbr.2009.12.001.

Taylor, L. L., J. R. Leake, J. Quirk, K. Hardy, S. A. Banwart, and D. J. Beerling (2009), Biological weathering and the long-term carbon cycle: Integrating mycorrhizal evolution and function into the current paradigm, *Geobiology*, *7*(2), 171–191, doi:10.1111/j.1472-4669.2009.00194.x.

Turpault, M.-P., and L. Trotignon (1994), The dissolution of biotite single-crystals in dilute Hno_3 at 24°C: Evidence of an anisotropic corrosion process of micas in acidic solutions, *Geochim. Cosmochim. Acta*, *58*(13), 2761–2775, doi:10.1016/0016-7037(94)90112-0.

van Breemen, N., R. Finlay, U. Lundström, A. G. Jongmans, R. Giesler, and M. Olsson (2000), Mycorrhizal weathering: A true case of mineral plant nutrition?, *Biogeochemistry*, *49*(1), 53–67, doi:10.1023/A:1006256231670.

Yuan, L., J. G. Huang, X. L. Li, and P. Christie (2004), Biological mobilization of potassium from clay minerals by ectomycorrhizal fungi and eucalypt seedling roots, *Plant Soil*, *262*(1–2), 351–361, doi:10.1023/B:PLSO.0000037055.67646.97.